Available online at www.sciencedirect.com
SCIENCE DIRECT
ELSEVIER
International Journal of Pharmaceutics 315 (2006) 158–166
INTERNATIONAL JOURNAL OF PHARMACEUTICS
www.elsevier.com/locate/ijpharm

Pharmaceutical Nanotechnology

A novel chitosan oligosaccharide–stearic acid micelles for gene delivery: Properties and in vitro transfection studies

Fu-Qiang Hu *, Meng-Dan Zhao, Hong Yuan, Jian You, Yong-Zhong Du *, Su Zeng

College of Pharmaceutical Sciences, Zhejiang University, Hangzhou 310031, PR China

Received 20 January 2006; received in revised form 10 February 2006; accepted 10 February 2006
Available online 6 March 2006

Abstract

Stearic acid (SA) grafted chitosan oligosaccharide (CSO) (CSO–SA), which was synthesized by an 1-ethyl-3-(3-dimethylaminopropyl)carbodiimide (EDC)-mediated coupling reaction, was demonstrated to form micelle like structure by self-aggregation in aqueous solution. The critical micelle concentration (CMC) of CSO–SA with 15.4% amino substituted degree of CSO was about 0.035 mg/ml. The micelles with 1 mg/ml CSO–SA concentration had 70.6 nm volume average hydrodynamic diameter with a narrow size distribution and 46.4 ± 0.1 mV surface potential. Due to the cationic property, the micelles could compact the plasmid DNA to form micelle/DNA complexes nanoparticles, which can efficiently protect the condensed DNA from enzymatic degradation by DNase I. The volume average hydrodynamic diameter of CSO–SA micelle/DNA complex increased from 203 nm to 318 nm and decreased to 102 nm due to the variation of zeta potential when the N/P ratio increased from 0.25 to 3.6 and from 3.6 to 58. The IC_{50} value of the CSO–SA micelle against A549 cells was 543.16 μg/ml, while the IC_{50} of Lipofectamine™ 2000 was about 6 μg/ml. The in vitro transfection efficiency of CSO–SA micelles was investigated by using plasmid DNA (pEGFP-C1). The transfection efficiency with CSO–SA/DNA (N/P ratio is 29) was increased with the post-transfection time (in 76 h), while the optimal transfection of Lipofectamine™ 2000/DNA was obtained at 24 h. The transfection of CSO–SA was not interfered in the presence of 10% fetal bovine serum, which showed remarkable enhancement effect. The optimal transfection efficiency of CSO–SA micelles in A549 cells was about 15%, which was higher than that of CSO (about 2%) and approach to that of Lipofectamine™ 2000 (about 20%). The low cytotoxic biodegradable CSO–SA micelles could be used as an effective DNA condensation carrier for gene delivery system.

Keywords: Non-viral vector; Chitosan oligosaccharide; Micelle; Transfection efficiency; Lipofectamine™ 2000

1. Introduction

Efficient gene transfer is a key factor in gene therapy. Two main types of vectors that are used in gene therapy are based on viral or non-viral gene delivery systems. Non-viral gene delivery systems have recently received increasing interest due to safety concerns with viral vectors (Kong et al., 2005; Salem et al., 2003). A number of non-viral gene delivery vectors including cationic liposome (Sellins et al., 2005; Pringle et al., 2005), nature and synthetic polymers (Son et al., 2004; Neu et al., 2005; Savic et al., 2003; Kang et al., 2005) have been introduced as alternatives against viral vectors due to their potential advantages of low immunogenicity and ease to preparation. Although the cationic liposomes have higher transfection efficiency comparing with cationic polymer, but the higher toxicity restrict their application for gene delivery system. On the other hand, cationic polymers are more stable than cationic lipids. However, compared to cationic liposome, the efficiency of gene delivery by cationic polymers is still relatively low.

As biodegradable, biocompatible, low immunogenicity and non-toxic material, chitosan and its derivatives have been widely accepted as a non-viral vector for gene delivery (Borchard, 2001; Mansouri et al., 2004). Chitosan is a cationic natural polysaccharide, it can be complexed with negatively charged DNA by ionic interactions, and protects DNA against DNase degradation and leads to its condensation (Cui and Mumper, 2001; Illum et al., 2001). However, its low transfection efficiency problem remains to be solved. For this target, various modifications of side chain of the chitosan and the optimizations of formulation have been performed (Kean et al., 2005; Yoo et al., 2005; Mao et al., 2005). Recent reports indicated that chitosan exhibited

* Corresponding authors. Tel.: +86 571 87217327; fax: +86 571 87217327.
E-mail addresses: hufq@zju.edu.cn (F.-Q. Hu), duyongzhong@zju.edu.cn (Y.-Z. Du).

0378-5173/$ – see front matter © 2006 Elsevier B.V. All rights reserved.
doi:10.1016/j.ijpharm.2006.02.026

dose-dependent blood compatibility and cell viability (Kojima et al., 2001). Such drawbacks of chitosan seem to relate with chemical and physical characteristics such as the deacetylation degree and molecular weight of chitosan (Lee et al., 1995). The chitosan with low molecular weight, namely chitosan oligosaccharide (CSO), has been focused for the gene delivery system (Richardson et al., 1999). As reported by other groups (Jeon and Kim, 2000; Chae et al., 2005), CSO is soluble in water and can be easily obtained by enzymatic degradation of chitosan and ultrafiltration separation. Moreover, CSO has reactive amino and hydroxyl groups, thus many CSO derivatives for pharmaceutical application can be obtained by chemically altering its properties under mild reaction conditions (Kim et al., 2005; Yokasan et al., 2004; Kwon et al., 2003). In particular, stearic acid (SA), an endogenous long-chain saturated fatty acid, was widely accepted for pharmaceutical use (Qiang et al., 2000; Hu et al., 2005). As a main composition of fat, stearic acid is biocompatible with low cytoxicity.

In this study, CSO was obtained by enzymatic degradation of chitosan and subsequently separation using ultrafiltration. SA was then chosen as hydrophobic segments to synthesize an amphiphilic grafted copolymer based on CSO. The properties of micelles formed by CSO–SA were investigated. The CSO–SA micelles were further used as plasimd DNA condensation agent. The properties of CSO–SA/DNA complex nanoparticles, DNA stability in CSO–SA/DNA complex nanoparticles, cytotoxicity and in vitro transfection efficiency of CSO–SA micelles were evaluated.

2. Materials and methods

2.1. Materials

Randomly 95% deacetylated chitosan (M_w = 450.0 K) was supplied by Yuhuan Marine Biochemistry Co., Ltd. (Zhejiang, China) and chitosanase was purchased from Chemical Industries Co., Ltd. (Japan). Stearic acid was purchased from Shanghai Chemical Reagent Co. Ltd. (China). 1-Ethyl-3-(3-dimethylaminopropyl)carbodiimide (EDC), 2,4,6-trinitrobenzene sulfonic acid (TNBS), and 3-(4,5-dimethylthiazol-2-yl)-2,5-diphenyl-tetrazolium bromide (MTT) were purchased from Sigma (St. Louis, MO, USA). Polysaccharide (Part Number: 2090-0100) was purchased from Polymer Laboratories Co., Ltd. (USA) and pyrene was purchased from Aldrich Chemical Co., Ltd. (USA). Lipofectamine^{TM} 2000 was supplied from Invitrogen Corporation (CA, USA). DNase I, Dulbecco's modified eagle's medium (DMEM) and trypsin-EDTA were purchased from Gibco BRL (Gaithersberg, MD, USA). Fetal bovine serum (FBS) was purchased from Sijiqing Biologic Co., Ltd. (Zhejiang, China). Ethanol and other chemicals were analytical grade and used without further purification.

2.2. Cell lines

A549 cells, human cell line derived from the respiratory epithelium cells, were obtained from Cell Resource Center of China Science Academe. The cells were cultured at 37 °C with 5% CO_2 and under fully humidified conditions. The culture medium was DMEM supplemented with 10% FBS, 100 units/ml penicillin, and 100 μg/ml streptomycin.

2.3. Plasmid DNA

Plasmid DNA (pEGFP-C1) encoding the enhanced GFP was used to assess transfection as well as expression efficiency. The plasmid DNA was donated from the first Affiliated Hospital, College of Medicine, ZheJiang University (Hangzhou, China). The plasmid DNA was amplified using Escherichia coli DH5a and purified using the Endo Free Qiagen kit (Qiagen, Valencia, CA, USA) to remove the bacterial endotoxins.

2.4. Preparation of CSO by enzymatic degradation of chitosan

A 3% chitosan solution was prepared by dispersing 15 g of chitosan in 500 ml of distilled water. After adding 6.25 ml of 36.5% (w/v) hydrochloric acid, the temperature of the mixture was raised up to 50 °C in a batch reactor, and 1 unit/ml chitosanase was added. The reaction time of hydrolysis was controlled by molecular weight measurement of chitosan, which performed by viscosity method. The reaction mixture was then centrifugated for 10 min at 4000 rpm. The obtained supernatant was filtered by filter with 0.45 μm pole size, and then ultrafiltered by various molecular weight cut off (NMWCO) ultrafiltration membrane (Millipore Labscale TFF system, Millipore Co., USA). The low molecular weight chitosan, chitosan oligosaccharide (CSO) were obtained by lyophilization.

The molecular weight of final chitosan oligosaccharide (CSO) was determined by gel permeation chromatography (GPC) with TSK-gel column (G3000SW, 7.5 mm × 30 cm I.D.) at 25 °C. The weighted lyophilized powder of CSO was dissolved in acetate buffer solution (pH 6.0) and the final concentration was adjusted to 1.0 mg/ml. Then, 10 μl of the sample was chromatographed using acetate buffer solution (pH 6.0) as the elution buffer and a flow rate of 0.8 ml/min.

Master samples of polysaccharide with different molecular weight (M_w = 5.9, 11.8, 22.8, 47.3, 112, 212 K) were dissolved in acetate buffer solution (pH 6.0), and their final concentration were set to 0.5 mg/ml. Calibration was performed by means of polysaccharide samples using the integral molecular weight distribution method.

2.5. Synthesis of CSO–SA

SA grafted CSO copolymer (CSO–SA) was synthesized via the reaction of carboxyl group of SA with amine group of CSO in the presence of 1-ethyl-3-(3-dimethylaminopropyl) carbodiimide (EDC). Briefly, CSO (0.4 g) was dissolved in 30 ml distilled water and stearic acid (0.5 g) was dissolved in 20 ml ethanol by sonicate treatment (Sonic Purger CQ250, Academy of Shanghai Shipping Electric Instrument) in water bath at room temperature for 30 s, respectively. EDC (2 g) was added to the CSO solution, under mechanic stirring with 400 rpm at room temperature. The mixture of CSO solution containing EDC was

heated up to 90 °C under vigorous stirring accompanied by dropwise addition of 20 ml of stearic acid solution. The reaction mixture was stirred at 90 °C for 5 h, then the reaction mixture was cooled to room temperature and the reaction was continued for further 24 h under stirring. After the reaction, the reaction mixture was dried in a vacuum oven at 50 °C. The dried product was dispersed in 20 ml ethanol. The suspension was then filtered with 0.22 μm millipore filter to collect the precipitate and the precipitate was further washed with 10 ml ethanol twice to remove the unreacted SA. After this process, the precipitate was dissolved in 20 ml distilled water, and then dialyzed by using dialysis membranes (MWCO: 8 kDa, Spectrum Laboratories, Laguna Hills, CA) against distilled water for 24 h with successive exchange of fresh distilled water in order to remove other water-soluble by-products. The dialyzed product was lyophilized.

IR spectra of resulted products were measured by a 460-type spectrometer (Shimudza Co., Japan) to determine the chemical interaction between CSO and SA.

The degree of substitution, defined as the number of stearic acid groups per 100 amino groups of CSO, was determined by TNBS method (Andres and Martina, 1998).

2.6. Characterization of CSO–SA micelle

The CMC of synthesized CSO–SA was determined by fluorescence measurement using pyrene as a probe (Kalyanasundaram and Thomas, 1977). The fluorescence emission spectrums of pyrene were measured at varying concentration of CSO–SA solution with the range from 2.5×10^{-4} mg/ml to 2.5 mg/ml by using fluorometer (F-4000, HITACHI Co., Japan). The concentration of pyrene was controlled at 6×10^{-7} M. The slit openings were set at 5 nm (excitation) and 5 nm (emission). The excitation wavelength (λ_{ex}) was 336 nm and the spectra were accumulated with an integration time of 5 s/nm. The intensity ratio was calculated from the first (377 nm) and the third (395 nm) highest energy bands in the pyrene emission spectra.

The average hydrodynamic diameter and zeta potential of the micelles with 1 mg/ml of CSO–SA concentration were measured by dynamic light scattering using a Zetasizer (3000HS, Malvern Instruments Ltd., UK).

2.7. Preparation and Characterization of CSO–SA /DNA complex nanoparticles

Micelle solutions of CSO–SA with different concentration (25 mM sodium acetate buffer, pH 5.5) were firstly purified by 0.22 μm millipore filter. The stable CSO–SA/DNA complex nanoparticles with various N/P ratios (The N/P ratio was calculated from the number of unreacted free primary amines of CSO–SA and the number of phosphate groups of DNA) were prepared by mixing the appropriate volume of CSO–SA micelle solution and DNA solution (500 μg/ml) vortically for 30 s, and then standing for 30 min.

The average hydrodynamic diameter and zeta potential of CSO–SA/DNA complex nanoparticles were measured by dynamic light scattering using a Zetasizer (3000HS, Malvern Instruments Ltd., UK).

The morphological examinations of Plasmid DNA, CSO–SA micelle and CSO–SA/DNA complex nanoparticles were performed by atomic force microscopy (AFM) (SPA 3800N, SEIKO, Japan) using tapping mode and high resonant frequency (F_0 = 129 kHz) pyramidal cantilevers with silicon probes having force constants of 20 N/m. Scan speeds were set at 2 Hz. The samples were diluted with distilled water, and then dropped onto freshly cleaved mica plates, followed by vacuum drying during 24 h at 25 °C.

2.8. Gel retardation assay

Varying amounts of CSO–SA micelles and 1 μg of plasmid DNA (pEGFP-C1) were combined in different N/P ratios, and mixed with gentle vortexing. The mixtures were stand for 30 min at room temperature prior to analysis. Electrophoresis was then carried out with a current of 100 V for 20 min in TAE buffer solution (40 mM Tris–HCl, 1% (v/v) acetic acid, 1 mM EDTA). The retardations of the CSO–SA/DNA complexes with various N/P ratios were visualized by the staining of ethidium bromide.

2.9. DNase I protection assay

The DNase I protection assay of CSO–SA/DNA complexes was performed according to the report (Jeong and Park, 2002). The CSO–SA/DNA complexes with 3.6 and 29 of N/P ratios were incubated in a buffer solution (10 mM Tris–HCl, 150 mM NaCl, 1 mM $MgCl_2$, pH 7.4) containing 25 units of DNase I. The UV absorbance change at 260 nm was measured at different intervals by using a UV spectrophotometer (UV-1601, Shimadzu, Japan).

2.10. In vitro transfection of A549 cells

A549 Cells were seeded 24 h into 24-well plates at a density of 2×10^5 cells/well in 1 ml of complete medium (DMEM containing 10% FBS, supplemented with 2 mM L-glutamate, 100 U/ml penicillin and 100 μg/ml streptomycin) prior to transfection. Before transfection experiments, the medium in each well was replaced with 0.5 ml fresh culture medium with or without FBS at pH 6.5, 7.0, 7.2 or 7.5. The different amount of complexes (CSO–SA/DNA (N/P ratio is 29) or CSO/DNA) equivalent to 1 μg of DNA(pEGFP-C1) were added to each well, and incubated with cells for initial 6 h. The medium was then replaced with 1 ml of fresh complete medium, and the incubation was continued for further 7–76 h at 37 °C. Transfection with Lipofectamine™ 2000/DNA complexes was performed as positive controls according to the manufacture's protocol. Briefly, cells were incubated with Lipofectamine™ 2000/DNA complexes (1 μg DNA) in 0.5 ml of serum-free medium for 6 h, and further incubated with 1 ml of fresh complete medium for 7–76 h at 37 °C before the analysis for transfection efficiency. All transfection experiments were performed in triplicate.

For the fluorescence assay of transfection, the cells were harvested at different time by removing the media then adding

200 μl 1 × lysis buffer (Promega, Madison, IL, USA), leaving for 5–10 min and gently scraping off the plate. The cell lysate was centrifuged at 12,000 rpm for 5 min and the supernatant removed. A sample was assayed for fluorescence by using fluorometer (F-4000, HITACHI Co., Japan) (excitation: 488 nm; emission: 520 nm).

The optimal transfection efficiency was evaluated by using FACScan analysis. After 24–72 h incubation, cells were washed with cold PBS (Dulbecco's Phosphate buffered saline) and harvested by the addition of trypsin-EDTA solution. Finally, 1 ml of PBS was added and cells were centrifuged at 3000 × *g* for 4 min. The pellet was then resuspended in PBS containing 2% formalin and analyzed on a FACScan flow cytometer (BD Biosciences, USA). Determination of GFP positive events was performed by a standard gating technique. On the other hand, cells were also directly viewed under a fluorescence microscope (OLYMPUS America, Melville, NY).

2.11. In vitro toxicity assay

A549 cells were seeded in a 96-well plate at a seeding density of 10,000 cells per well in 0.2 ml of growth medium consisting of DMEM with 10% FBS and antibiotics. Cells were cultured at 37 °C for 24 h. The growth medium was then removed and growth medium containing the desired amount of CSO, CSO–SA micelles or Lipofectamine™ 2000 was added. The cells were further incubated for 48 h. After incubation, the metabolic activities of the cells were measured. A 100 μl of fresh growth medium containing 50 mg MTT was added to each well, and cells were incubated for 4 h. After the unreduced MTT and medium were removed, each well was washed with 100 μl of PBS and 180 μl of DMSO were then added to each well to dissolve the MTT formazan crystals. Plates were shaken for 20 min and the absorbance of formazan product was measured at 570 nm in a microplate reader (BioRad, Model 680, USA). Survival percentage was calculated as compared to mock-treated cells (100% survival) (Mosmann, 1983).

3. Results and discussion

3.1. Synthesis of CSO–SA

CSO was firstly prepared by hydrolysis of chitosan in the presence of chitosanase at 50 °C under the acid condition, and the CSO with narrow molecular weight distribution was obtained by ultrafiltrating with various molecular weight cut off ultrafiltration membrane. The final molecular weight of CSO was measured by gel permeation chromatography. The M_n (number average molecular weight), M_w (weight average molecular weight) and M_w/M_n (the polydispersity) of CSO used in this research were 9.95, 18.7 and 1.88 K. It was confirmed that the obtained CSO was easily dissolved in the distilled water at the pH below 7.4.

CSO–SA grafted copolymer was then synthesized via the reaction of carboxyl group of SA with amine group of CSO in the presence of water-soluble 1-ethyl-3-(3-dimethylaminopropyl)carbodiimide (EDC). The water-soluble EDC is called 'zero-length' cross-linker because the amide linkages are formed without leaving a spacer molecule (Pieper et al., 2000). EDC reacts with the carboxyl group of stearic acid to form an active ester intermediate, which can further react with a primary amine of CSO to form an amide bond. The remained EDC and by-product (isourea) can easily remove by dialysis with water (Lee et al., 1998).

To investigate the binding between SA and CSO, IR spectra (data not shown) of CSO, SA and CSO–SA were investigated. It is clear that the peaks of amide bands I and II of CSO are appeared at 1620 cm^{-1} and 1510 cm^{-1}, respectively. The new peaks of amide bands I and II were observed at 1640 cm^{-1} and 1560 cm^{-1} in the spectra of CSO–SA, respectively. The shifted peaks of amide bands I and II were caused by the amide band between CSO and SA. On the other hand, no absorption peak of the carboxyl groups of SA (1700 cm^{-1}) was found in the IR spectra of CSO–SA.

The degree of amino substitution of prepared CSO–SA was about 15.4% from the determination by 2,4,6-trinitrobenzene sulfonic acid method.

3.2. Characteristics of CSO–SA micelle

CSO–SA micelles were easily prepared by dispersing CSO–SA in distilled water with ultrasonic due to its inherent self-aggregation in aqueous environment. In general, the hydrophobic SA segments of CSO–SA molecular were self-associated into a hydrophobic core, while the hydrophilic CSO segments were pushed into water phase surrounding the core. The aggregation behavior of CSO–SA in aqueous media was investigated by fluorometry with pyrene as a fluorescent probe (Kalyanasundaram and Thomas, 1977). The CMC value of CSO–SA in distilled water was determined to be about 0.035 mg/ml, which is lower than that of low molecular weight surfactants in water (Riess, 2003).

Fig. 1 shows the distributions of hydrodynamic diameter and zeta potential of CSO–SA micelle with 1 mg/ml of CSO–SA concentration. The CSO–SA micelle with 1 mg/ml of CSO–SA concentration had about 70.6 nm of volume average hydrodynamic diameter and 46.4 mV of average of zeta potential.

3.3. Characteristics of CSO–SA/DNA complexes

Due to the positive charge, the CSO–SA micelle was used to condense the DNA forming CSO–SA/DNA complex nanoparticles. The CSO–SA/DNA complex nanoparticles with N/P ratio from 0.25 to 58 were prepared by mixing the appropriate volume of CSO–SA micelle solution and DNA solution. The variations of volume average hydrodynamic diameter and zeta potential of CSO–SA/DNA complex nanoparticles against N/P ratio are shown in Fig. 2. It is clear that the volume average hydrodynamic diameter of CSO–SA/DNA complex nanoparticles increased from 203 nm to 318 nm as the N/P ratio of CSO–SA/DNA complexes increased from 0.25 to 3.6. The increase of hydrodynamic diameter of the complexes was due to the decrease of complex stability caused by the decrease in absolute value of zeta

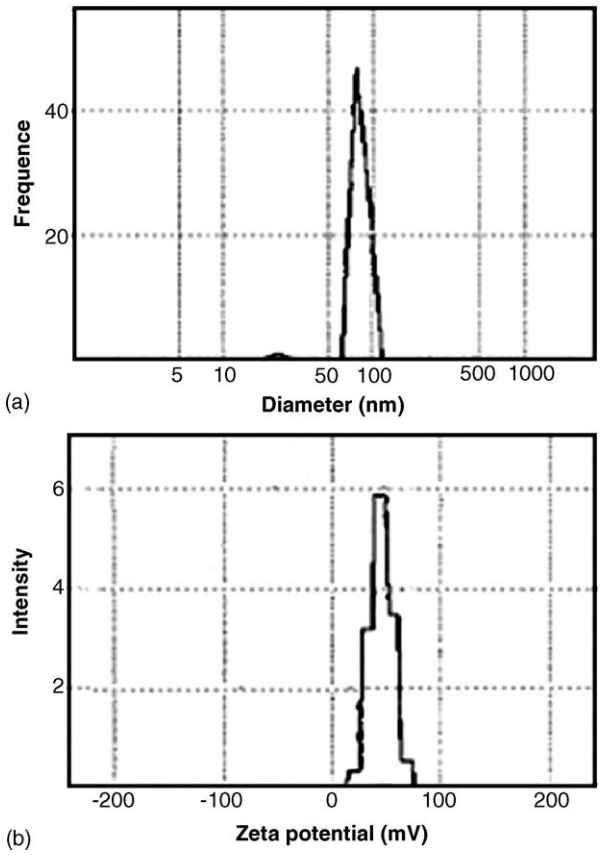

Fig. 1. The size distribution (a) and zeta potential (b) distribution of CSO–SA micelle with 1 mg/ml CSO–SA concentration.

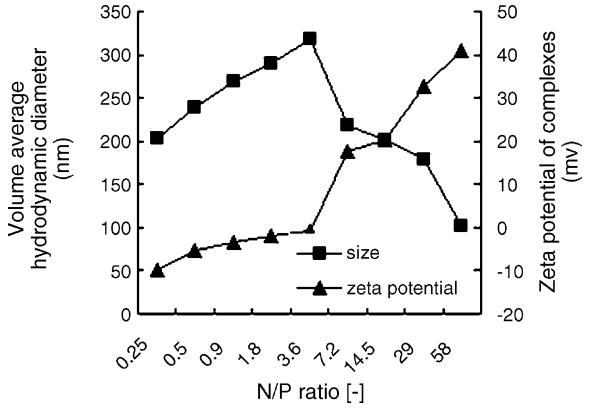

Fig. 2. The variations of volume average hydrodynamic diameter and zeta potential of CSO–SA/DNA complex nanoparticles against N/P ratio.

potential. Notice the zeta potential was increased from −10 mV to 0 mV as the N/P ratio increased from 0.25 to 3.6 (Fig. 2). On the other hand, the hydrodynamic diameter decreased from 318 nm to 102 nm when the N/P ratio further increased to 58.

Fig. 3(a)–(c) shows the image of atomic force microscopy for CSO–SA micelles, plasmid DNA, and CSO–SA/DNA complex nanoparticles, respectively. From Fig. 3(a) the quasi-spherical shape of CSO–SA micelle was observed, and the linear DNA structures were observed in Fig. 3(b). Furthermore, Fig. 3(c) showed ball or elliptical spherical shape of CSO–SA/DNA complexes, which indicated the linear DNA molecules were compacted by CSO–SA micelles to form complex nanoparticles.

The DNA condensation capacity of CSO–SA micelles was also analyzed at different N/P ratios of CSO–SA/DNA by a gel retardation assay using an agarose gel electrophoresis. Fig. 4 shows the gel retardation results of the complexes with N/P ratio from 0.25 to 58. The complete retardation of the complexes can be seen when the N/P ratio was above 3.6, which suggested CSO–SA micelles and plasmid DNA started to form tight complexes.

3.4. DNase I protection assay

Protection of plasmid DNA from nucleases is one of the crucial factors for efficient gene delivery in vivo as well as in vitro (Katayose and Kataoka, 1998). The effect of protection to plasmid DNA in CSO–SA/DNA complexes from DNase I degradation was examined using DNase I as a model enzyme. Increasing the UV absorbance value at 260 nm with incubation time reveals the degradation of DNA backbone. Fig. 5 shows naked plasmid DNA was significantly degraded in 5 min, whereas the complexed with CSO–SA polymeric micelles, the condensed plasmid DNA was efficiently protected from the attack of DNase

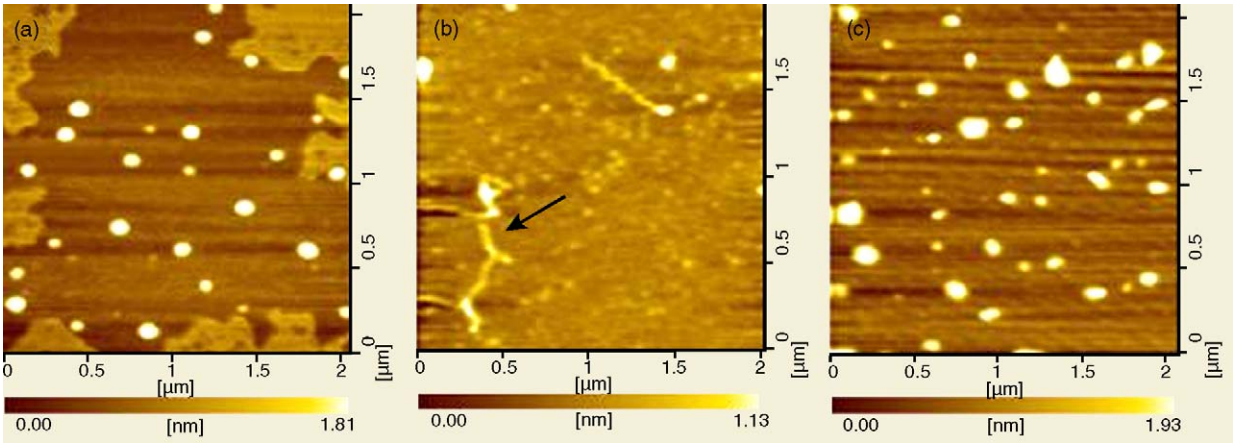

Fig. 3. Images of atomic force microscopy: (a) CSO–SA micelles; (b) free plasmid DNA; (c) CSO–SA/DNA complexes (N/P = 29).

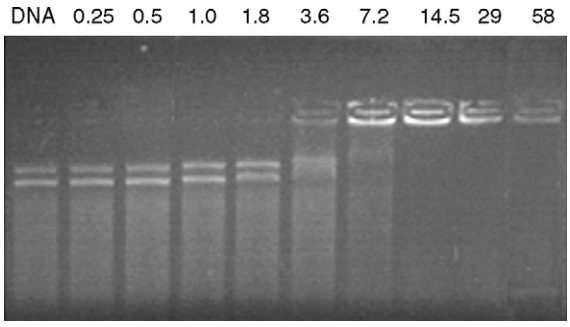

Fig. 4. Gel retarding analysis of CSO–SA/DNA complex nanoparticles. Lane 1 is naked DNA; lanes 2–9 are CSO–SA/DNA complex nanoparticles with N/P ratio of 0.25, 0.5, 1.0, 1.8, 3.6, 7.2, 14.5, 29 and 58, respectively.

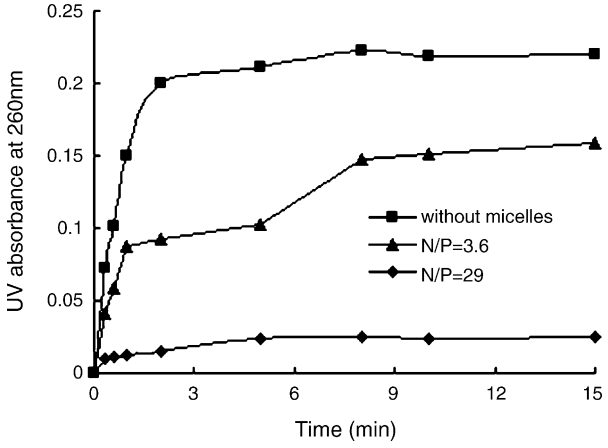

Fig. 5. Variation of UV absorbances at 260 nm against reaction time in DNase degradation experiments with or without CSO–SA micelles.

I (N/P ratio of 29). Some extent of degradation could be observed at the N/P ratio of 3.6, at which the complexes having a less compact structure was fail to give a full protection of DNA from the enzymatic attack. This result is consistent with the gel retardation result of Fig. 4, in which the DNA was not fully condensed with the polymeric micelles at the N/P ratio of 3.6.

3.5. Cell viability

Some studies showed that cytotoxicity was originated from the structural destabilization of lipid membranes by polycations, but the process of cationic polymer-mediated cytotoxicity is still unclear. Herein the effects of CSO, CSO–SA micelles and Lipofectamine™ 2000 on cell viability were investigated by using A549 cells and MTT assay. The results showed slightly decreasing in viability when the cells were cultured with either CSO or CSO–SA containing 1 μg DNA; while cells demonstrate reduced cell viability following their incubation with the Lipofectamine™ 2000. The IC_{50} of CSO and CSO–SA were measured to be 844.36 μg/ml and 543.16 μg/ml, respectively, while IC_{50} of Lipofectamine™ 2000 was about 6 μg/ml.

3.6. In vitro transfection of complex nanoparticles

The intracellular expression of DNA (pEGFP-C1) genes following in vitro transfection experiment was examined using a fluorescence microscope and FACScan flow cytometer. The effect of serum on the transfection was examined by fluorescence intensity assay. It was confirmed that the level of transfection of CSO–SA/DNA complex was increased in the presence of 10% serum-containing medium. This may be due to cell viability being optimal for transfection under this circumstance. However, Lipofectamine™ 2000/DNA complexes give the lower transfection activity in 10% serum. This indicates that CSO–SA is more compatible for transfection in vivo than Lipofectamine™ 2000.

The effect of post-transfection time on the transfection was investigated (the pH of culture medium was 7.2) as well. All experiments were repeated three times. Fig. 6(A) shows that a sharp increase in Lipofectamine™ 2000/DNA expression was observed in 24 h post-transfection. Maximum fluorescence intensity was obtained at 24 h. After 24 h, the transfection and DNA (pEGFP-C1) expression decreased rapidly. On the other hand, when the CSO–SA was used as a transfection carrier (the culture medium containing 10% FBS, N/P ratio is 29), the fluorescence intensity was increased with the post-transfection time (until 76 h). After 76 h cellular incubation with CSO–SA/DNA, the cells became multi-layers in the well due to the cellular growth, and the transfection experiments were stopped. The decrease of transfection after 24 h in the case of Lipofectamine™ 2000 may be due to its higher cytotoxicity. The increased transfection of CSO–SA in 76 h and the relatively lower transfection may be related to the lower release rate

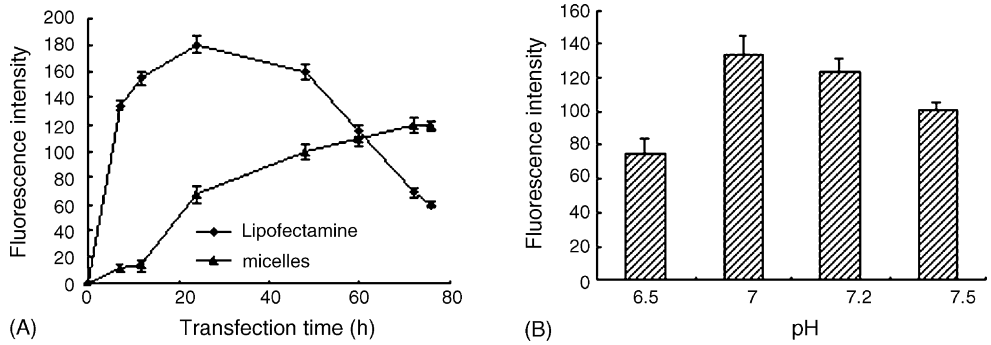

Fig. 6. Effects of post-transfection time (A) and pH of transfection medium (B) on transfection (A shows the transfection of CSO–SA/DNA complexes with N/P = 29 and Lipofectamine™ 2000/DNA complexes, and B shows the transfection of CSO–SA/DNA complexes with N/P = 29).

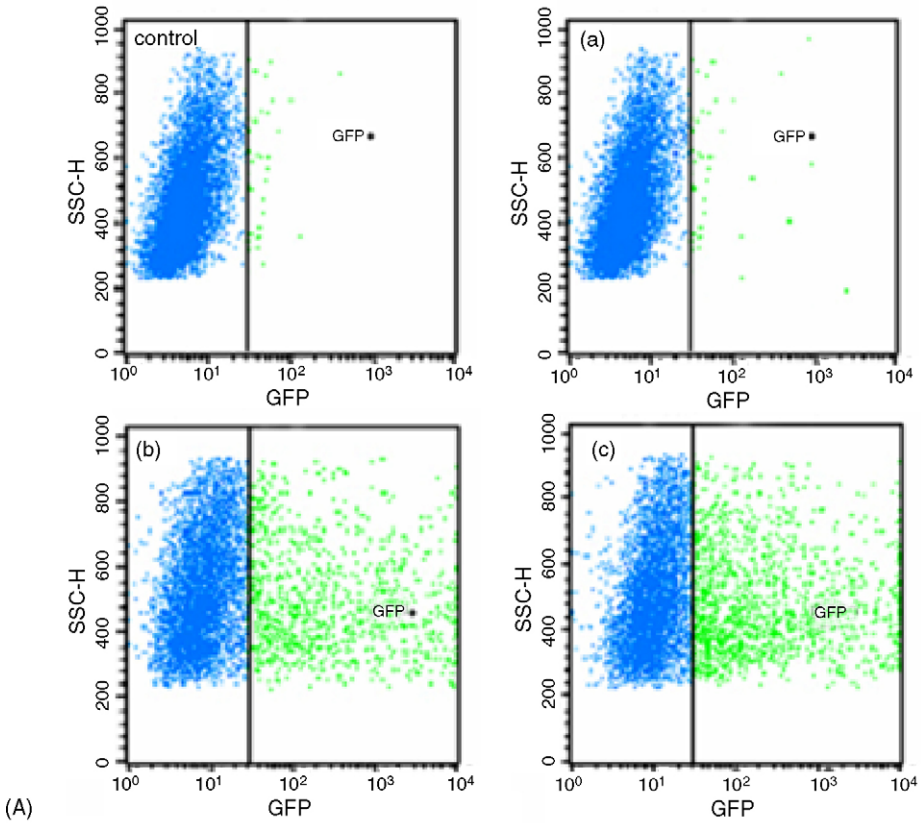

(A)

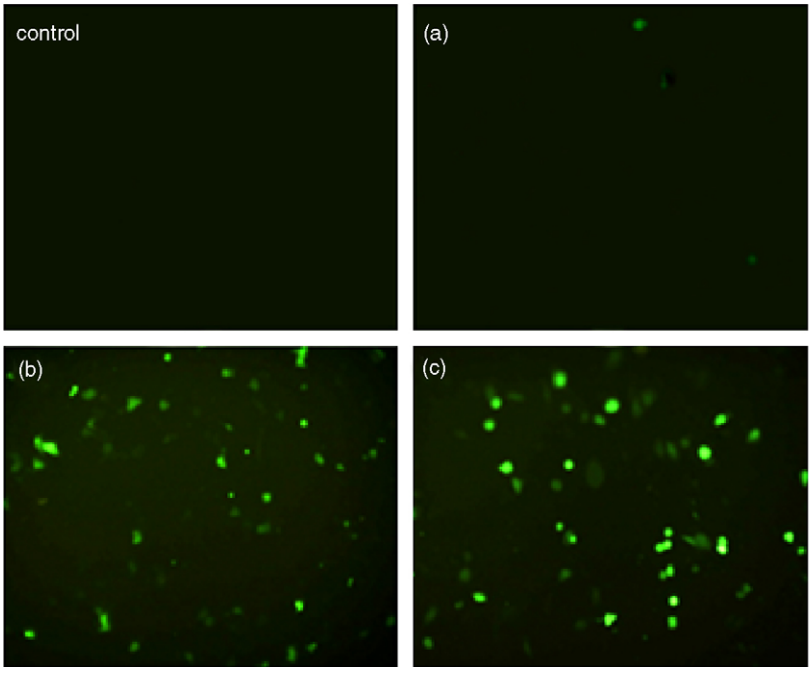

(B)

Fig. 7. Flow cytometry analysis (A) and fluorescence image observations (B) for DNA (pEGFP-C1) expression in A549 cells cultures using free plasmid DNA (control), CSO/DNA (a), CSO–SA/DNA (b) and Lipofectamine™ 2000/DNA (c).

of DNA from CSO–SA and the lower cytotoxicity than that of Lipofectamine™ 2000.

Fig. 6(B) shows the effect of the pH of culture medium on the transfection of CSO–SA/DNA. When the pH of culture medium increased from 6.5 to 7.0, the transfection was increased significantly. The transfection indicated slightly decrease as the pH of culture medium increased from 7.0 to 7.5. These results were agreed with the results reported by Ishii et al. (2001). The amount

of cell uptake was correlated to the level of transfection activity except for medium of pH 6.5. The slight decrease of transfection as the pH of culture medium increased from 7.0 to 7.5 might be due to the lower zeta potential and consequently the lower ability of cellular up-taken. When pH was altered from 7.0 to 6.5, an analysis of zeta potential showed increase in the positive charge of the complexes (data not shown). In the case of latter, the stronger protonation of amino groups of CSO–SA might reduce the escape ability of CSO–SA/DNA nanoparticles from endosome.

From above results, we further analyzed the optimal intracellular expression of DNA (pEGFP-C1) genes following in vitro transfection experiment by using FACScan flow cytometer and a fluorescence microscope. Fig. 7(A) shows the transfection efficiency of CSO/DNA (72 h), CSO–SA/DNA (N/P ratio is 29, post-tranfection time is 72 h) and Lipofectamine™ 2000/DNA complexes (24 h) by using FACScan flow cytometer. At the dose of 1 μg of DNA/well, cells transfected by the CSO–SA/DNA complexes reached about 15% which a little lower than that achieved by Lipofectamine™ 2000/DNA (about 20%) complexes at the same dose as control, while it was much higher than that of CSO/DNA (about 2%). Fig. 7(B) presents the fluorescence images of gene expression for CSO/DNA, CSO–SA/DNA and Lipofectamine™ 2000/DNA complexes. Fluorescence was not detected in A549 cells treated with naked plasmid DNA alone (data not shown), which means that the plasmid DNA had not migrated to localize within the cells. From this study, it is clear that pEGFP-C1 proteins were expressed in cells transfected with both CSO–SA/DNA and Lipofectamine™ 2000/DNA complexes. The high transfection of CSO–SA/DNA complexes than CSO/DNA may be relates with the specific structure. The amphiphilic graft copolymer composed of CSO as a backbone and SA as graft was expected to have a core-shell structure composed of hydrophobic SA segments as an internal core and cationic CSO as a surrounding corona. Due to the structure of longer main chain of CSO and shorter graft chain of SA in CSO–SA, a core-shell structured CSO–SA micelle with some SA "minor core" near the shell of micelle is considerable, which may favor the escape of CSO–SA/DNA complex from endosome. On the other hand, most of A549 cells were kept the shuttle like form after the CSO–SA-mediated gene expression, whereas a number of rotund cells were observed after the Lipofectamine™ 2000-mediated gene expression. The form change of cells may relate with the cytotoxic of material.

4. Conclusion

In summary, we demonstrated that the hydrophobic modified CSO, CSO–SA could self-aggregated to form micelle like structure in aqueous solution, and it indicated efficient ability to condense the plasmid DNA to form CSO–SA complex nanoparticles, which can efficiently protect the condensed DNA from enzymatic degradation by DNase I. The in vitro transfection experiment showed the optimal transfection efficiency of CSO–SA micelle in A549 cells was higher then that of CSO, and comparable with Lipofectamine™ 2000. The presence of 10% fetal bovine serum increased the transfection ability of CSO–SA. On the other hand, the cytotoxicity of CSO–SA was highly lower than that of Lipofectamine™ 2000. The low cytotoxicity of the present CSO–SA micellar vector, having an unhampered superior DNA condensation capacity, may be beneficial for non-virus gene transfer carrier.

Acknowledgements

We thank the financial supports of the National Nature Science Foundation of China under contract 30472101 and the Nature Science Foundation of Zhejiang province under contract M303817.

References

Andres, B.S., Martina, E.K., 1998. Mucoadhesive polymers as platforms for peroral peptide delivery and absorption: synthesis and evaluation of different chitosan–EDTA conjugates. J. Control. Release 50, 215–223.

Borchard, G., 2001. Chitosans for gene delivery. Adv. Drug Deliv. Rev. 52, 145–150.

Chae, S.Y., Jang, M.K., Nah, J.W., 2005. Influence of molecular weight on oral absorption of water soluble chitosans. J. Control. Release 102, 383–394.

Cui, Z., Mumper, R.J., 2001. Chitosan-based nanoparticles for topical genetic immunization. J. Control. Release 75, 409–419.

Hu, F.Q., Jiang, S.P., Du, Y.Z., Yuan, H., Ye, Y.Q., Zeng, S., 2005. Preparation and characterization of stearic acid nanostructured lipid carriers by solvent diffusion method in an aqueous system. Colloids Surf. B: Biointerfaces 45, 167–173.

Illum, L., Jabbal-Gill, I., Hinchcliffe, M., Fisher, A.N., Davis, S.S., 2001. Chitosan as a novel nasal delivery system for vaccines. Adv. Drug Deliv. Rev. 51, 81–96.

Ishii, T., Okahata, Y., Sato, T., 2001. Mechanism of cell transfection with plasmid/chitosan complexes. Biochim. Biophys. Acta 1514, 51–64.

Jeon, Y.J., Kim, S.K., 2000. Production of chitosan oligosaccharides using an ultrafiltration membrane reactor and their antibacterial activity. Carbohyd. Polym. 41, 133–141.

Jeong, J.H., Park, T.G., 2002. Poly(L-lysine)-g-poly(D,L-lactic-*co*-glycolic acid) micelles for low cytotoxic biodegradable gene delivery carriers. J. Control. Release 82, 159–166.

Kalyanasundaram, K., Thomas, J.K., 1977. Environmental effects on vibronic band intensities in pyrene monomer fluorescence and their application in studies of micellar systems. J. Am. Chem. Soc. 99, 215–220.

Kang, H.C., Kim, S., Lee, M., Bae, Y.H., 2005. Polymeric gene carrier for insulin secreting cells: poly(L-lysine)-g-sulfonylurea for receptor mediated transfection. J. Control. Release 105, 164–176.

Katayose, S., Kataoka, K., 1998. Remarkable increase in nuclease resistance of plasmid DNA through supramolecular assembly with poly(ethylene glycol)-poly(L-lysine) block copolymer. J. Pharm. Sci. 87, 160–163.

Kean, T., Roth, S., Thanou, M., 2005. Trimethylated chitosans as non-viral gene delivery vectors: cytotoxicity and transfection efficiency. J. Control. Release 103, 643–653.

Kim, K.Y., Kwon, S.L., Park, J.H., Chung, H., Jeong, S.Y., Kwon, I.C., 2005. Physicochemical characterizations of self-assembled nanoparticles of glycol chitosan–deoxycholic acid conjugates. Biomacromolecules 6, 1154–1158.

Kojima, K., Okamoto, Y., Miyatake, K., 2001. Optimum dose of chitin and chitosan for organization of non-woven fabric in the subcutaneous tissue. Carbohyd. Polym. 46, 235–239.

Kong, H.J., Liu, J.D., Riddle, K., Matsumoto, T., Leach, K., Mooney, D.J., 2005. Non-viral gene delivery regulated by stiffness of cell adhesion substrates. Nat. Mater. 4, 460–464.

Kwon, S., Park, J.H., Chung, H., Kwon, I.C., Jeong, S.Y., Kim, I.S., 2003. Physicochemical characteristics of self-assembled nanoparticles based on glycol chitosan bearing 5 beta-cholanic acid. Langmuir 19, 10188–10193.

Lee, K.Y., Ha, W.S., Park, W.H., 1995. Blood compatibility and biodegradability of partially *N*-acylated chitosan derivatives. Biomaterials 16, 1211–1216.

Lee, K.Y., Kwon, I.C., Kim, Y.H., Jo, W.H., Jeong, S.Y., 1998. Preparation of chitosan self-aggregates as a gene delivery system. J. Control. Release 51, 213–220.

Mansouri, S., Lavigne, P., Corsi, K., 2004. Chitosan-DNA nanoparticles as non-viral vectors in gene therapy: strategies to improve transfection efficacy. Eur. J. Pharm. Biopharm. 57, 1–8.

Mao, S.R., Shuai, X.T., Unger, F., Wittmar, M., Xie, X.L., Kissel, T., 2005. Synthesis, characterization and cytotoxicity of poly(ethylene glycol)-graft-trimethyl chitosan block copolymers. Biomaterials 26, 6343–6356.

Mosmann, T., 1983. Rapid colorimetric assay for cellular growth and survival: application to proliferation and cytotoxicity assays. J. Immunol. Methods 65, 55–63.

Neu, M., Fischer, D., Kissel, T., 2005. Recent advances in rational gene transfer vector design based on poly(ethylene imine) and its derivatives. J. Gene. Med. 7, 992–1009.

Pieper, J.S., Hafmans, T., Veerkamp, J.H., 2000. Development of tailor-made collagen-glycosaminoglycan matrices: EDC/NHS crosslinking, and ultrastructural aspects. Biomaterials 21, 581–593.

Pringle, I.A., Raman, S., Sharp, W.W., Cheng, S.H., Hyde, S.C., Gill, D.R., 2005. Detection of plasmid DNA vectors following gene transfer to the murine airways. Gene Ther. 12, 1206–1214.

Qiang, Z., Yie, G.Q., Li, Y., 2000. Studies on the cyclosporin A loaded stearic acid nanoparticles. Int. J. Pharm. 200, 153–159.

Richardson, S.C.W., Kolbe, H.J.V., Duncan, R., 1999. Potential of low molecular mass chitosan as a DNA delivery system: biocompatibility, body distribution and ability to complex and protect DNA. Int. J. Pharm. 178, 231–243.

Riess, G., 2003. Micellization of block copolymers. Prog. Polym. Sci. 28, 1107–1170.

Salem, A.K., Searson, P.C., Leong, K.W., 2003. Multifunction nanorods for gene delivery. Nat. Mater. 2, 668–671.

Sellins, K., Fradkin, L., Liggitt, D., Dow, S., 2005. Type I interferons potently suppress gene expression following gene delivery using liposome-DNA complexes. Mol. Ther. 12, 451–459.

Son, S.H., Chae, S.Y., Choi, C.Y., Kim, M.Y., Ngugen, V.G., Jang, M.K., Nah, J.W., 2004. Preparation of a hydrophobized chitosan oligosaccharide for application as an efficient gene carrier. Macromol. Res. 12, 573–580.

Savic, R., Luo, L.B., Eisenberg, A., Maysinger, D., 2003. Micellar nanocontainers distribute to defined cytoplasmic organelles. Science 300, 615–618.

Yoo, H.S., Lee, J.E.H.C., Kwon, I.C., Jeong, S.Y., 2005. Self-assembled nanoparticles containing hydrophobically modified glycol chitosan for gene delivery. J. Control. Release 103, 235–243.

Yokasan, R., Matsusaki, M., Akashi, M., Chirachanchai, S., 2004. Controlled hydrophobic/hydrophilic chitosan: colloidal phenomena and nanosphere formation. Colloid Polym. Sci. 282, 337–342.